

**Awake <sup>18</sup>F-FDG PET imaging of memantine-induced brain activation and test-retest in freely running mice.**

Alan Miranda,<sup>1†</sup> Dorien Glorie,<sup>1</sup> Daniele Bertoglio,<sup>1</sup> Jochen Vleugels,<sup>2</sup> Guido De Bruyne,<sup>2</sup> Sigrid Stroobants,<sup>1,3</sup> Steven Staelens,<sup>1</sup> Jeroen Verhaeghe<sup>1\*</sup>

<sup>1</sup>Molecular Imaging Center Antwerp, University of Antwerp, Universiteitsplein 1, 2610 Antwerp, Belgium

<sup>2</sup>Product Development, University of Antwerp, Antwerp, Belgium

<sup>3</sup>University Hospital Antwerp, Wilrijkstraat 10, 2650 Antwerp, Belgium

\*Campus Drie Eiken, Universiteitsplein 1, D.UC.057, 2610 Wilrijk, Belgium,  
jeroen.verhaeghe@uantwerpen.be, tel: +32652818, fax: +32652774

† Campus Drie Eiken, Universiteitsplein 1, D.UC.057, 2610 Wilrijk, Belgium,  
alan.mirandamenchaca@uantwerpen.be, tel: +32652818, fax: +32652774, PhD Student

Manuscript word count: 5235

This work was supported by a Research Project (G0A8517N) and Research Grant (1520217N) from the Research Foundation – Flanders (FWO).

Running title: Reproducibility of awake mice brain PET

## ABSTRACT

Positron emission tomography (PET) scans of the mouse brain are usually performed with anesthesia to immobilize the animal. However, it is desirable to avoid the confounding factor of anesthesia in mouse-brain response. **Methods:** We develop and validate brain PET imaging of awake, freely moving mice. Head-motion tracking is performed using radioactive point source markers and we use the tracking information for PET-image motion correction. Regional <sup>18</sup>F-Fluorodeoxyglucose (<sup>18</sup>F-FDG) brain uptake in a test, retest, and memantine challenge study was performed in awake (n=8) and anesthetized (n=8) C57BL/6 mice. An awake uptake period was considered for the anesthesia scans. **Results:** Awake (motion corrected) PET images showed an <sup>18</sup>F-FDG uptake pattern comparable to the pattern of anesthetized mice. The test-retest variability (represented by the intraclass correlation coefficient (ICC)) of the regional standardized uptake value (SUV) quantification in the awake images (0.424-0.555) was marginally lower compared to anesthesia images (ICC, 0.491-0.629) over the different regions. The increased memantine-induced <sup>18</sup>F-FDG uptake was more pronounced in awake (+63.6%) than in anesthesia (+24.2%) animals. Additional behavioral information, acquired during awake scans, showed increased motor activity on a memantine challenge (total distance travelled,  $18.2 \pm 5.28$  m) compared to test-retest ( $6.49 \pm 2.21$  m). **Conclusions:** The present method enables brain PET imaging on awake mice, thereby avoiding the confounding effects of anesthesia on the PET reading. It allows the simultaneous measurement of behavioral information during PET acquisitions. The method does not require any additional hardware, and it can be deployed in typical high-throughput scan protocols.

## INTRODUCTION

Small-animal positron emission tomography (PET) is performed under anesthesia to ensure immobilization of the animal and to avoid motion artifacts in the images. However, studies have indicated that anesthetics can interfere with the uptake of several PET radiotracers through the alteration of such physiological parameters as cerebral blood flow, body temperature, and heart rate (1-3). Physical restraint of the awake animal during the PET acquisition has been proposed to circumvent these issues (4). Unfortunately, immobilization stress also affects the uptake of such radiotracers as <sup>18</sup>F-Fluorodeoxyglucose (<sup>18</sup>F-FDG) (5) and <sup>11</sup>C-Raclopride (6). Given these confounding factors, it is desirable to perform PET acquisitions on freely moving animals, to ensure an unaffected brain response.

Several methods have been proposed for obtaining PET scans of the brain of freely moving animals. Schulz, et al. (7) surgically fixed a miniaturized PET scanner to the rat skull. An approach by Kyme, et al. (8) used a commercially available PET scanner to perform PET acquisitions with minimal restraint. In the latter method, an optical device tracked the motion of the rat head during the acquisition and motion correction was subsequently applied to the images. Our group developed this method further, replacing optical motion tracking with a point source tracking (PST) method in which radioactive markers are fixed to the head of the rat to measure its movement (9). The PST method does not require any hardware other than the PET scanner, and it allows tracking to be performed throughout the entire field-of-view (FOV), regardless of animal pose or scanner-bore size.

Earlier studies have been based only on PET imaging performed in awake rats, although transgenic models commonly used in neuroscience are more widely available for mice (10). For this reason, we report on the adaptation of the PST method to track head motion in freely moving mice during PET acquisitions. Compared to rats, the space available on the mouse head to fix the point sources is limited. In addition,

the motion range and speed of mice is greater than in rats. These aspects will be considered when adapting the tracking algorithm for mice imaging.

In this study, we compare the performance of awake imaging using PST versus anesthesia. To this end, <sup>18</sup>F-FDG was used to perform PET scans in a group of anesthetized mice undergoing an awake tracer uptake period, as well as in a group of mice scanned in an awake state. Test-retest and memantine-induced brain activation studies (11) were performed in both groups. Given the irreversible uptake of <sup>18</sup>F-FDG we expect to observe similar brain uptake in both groups, as both groups undergo similar awake tracer uptake periods. The memantine challenge was included as the induced increased locomotion (12) represents a challenge for the motion tracking algorithm. In addition, it allowed to assess the ability of the awake imaging to detect memantine induced alterations in brain uptake as well as in behavior.

## MATERIAL AND METHODS

### PET Scanner

Scans were performed using two Siemens Inveon scanners (Siemens Medical Solutions, Inc., Knoxville, USA). The axial FOV is 12.7 cm in length, with a transaxial diameter of 10 cm. The scanner has a spatial resolution of 1.5 mm at the center of the FOV (CFOV), which increases in the radial direction to 3.5 mm at the edge of the FOV (13) due to the parallax effect. Images were reconstructed in a 128×128×159 matrix, with a voxel size of 0.776×0.776×0.796 mm in the *x*, *y*, and *z* directions, respectively.

### Mouse Holder

A cylindrical animal holder was designed to fit inside the Inveon scanner while keeping the mouse inside the scanner FOV (Fig. 1). The cylinder case has a length of 16.5 cm and a diameter of 10 cm. Inside the cylinder, a horizontal platform of 10×9 cm allows movement of the mouse in all directions.

## **Point Source Tracking**

We previously validated the PST method (9) for tracking the head motion of an awake rat. Briefly, four radioactive point sources ( $\sim 1$  mm diameter) are glued onto the animal's head. Two point sources are fixed under each ear, one on the nasal bridge and one on top of the head on a light weight spacer made of foam paper. The activity of each point source was in the range 296-370 kBq. After the PET acquisition, the point sources are tracked in short time frame images (32 ms). Each short frame is reconstructed using list-mode reconstruction (14). Each image frame is processed sequentially to determine the position of the point sources. Probable point sources are calculated, after which the correct point sources are found by selecting those that minimize a similarity error score with respect to a predefined model. Once the point sources have been found in all short frames, the pose (position and orientation) of the animal head is calculated from the point source locations. Poses are verified by aligning the frame point sources to the rigid model. Frames with at least one point source with a distance larger than 2 mm from the rigid model were discarded. Finally, motion corrected PET images can be reconstructed. Compared to the rat head PST, the step where the similarity to ideal spheres was calculated for point sources (9) had to be replaced. Due to the higher mouse motion speed, the point sources were blurred and did not represent ideal spheres. Therefore, a new metric that only considers geometrical features, such as the position of the points with respect to other points, was included.

## **Image Reconstruction**

A list-mode ordered-subsets reconstruction (14) (16 subsets, 8 iterations) with spatial resolution modeling (15) was used for both motion-free (anesthesia) and motion corrected (awake) images. Awake images included event-by-event motion correction (16). Attenuation correction factors were calculated from the CT scan for the anesthetized animals and from the mouse body activity outline for the awake animals (17). In the latter method, the mouse body shape is estimated from the whole body uptake, which

is present along the entire body for  $^{18}\text{F}$ -FDG. Attenuation by the mouse body is therefore considered in motion corrected scans assuming a constant linear attenuation coefficient for soft tissue ( $0.097\text{ cm}^{-1}$ ) for the whole body. No scatter correction was performed. Dynamic reconstructions were performed as reconstructions of independent 2-minute frames, using the same algorithms used for static reconstructions.

### **Animal Preparation**

Animals were subdivided into two separate groups. One group of 8 mice (C57BL/6, Charles River, Lyon France,  $24.9 \pm 1.9\text{ g}$ , 18 weeks old) was scanned under anesthesia, and another group of 8 mice ( $24.6 \pm 1.4\text{ g}$ , 18 weeks old) received scans in the awake state. This group division was retained for all three acquisitions (test, retest, and memantine challenge scans) received by each animal. All animals were housed in a temperature-controlled room with a 12-hour light-dark cycle (food and water available ad libitum). The night before each scan, all animals were fasted for at least 12 hours with free access to water. Isoflurane gas anesthesia was used for procedures (5% induction, 2% maintenance). The experiments followed the European Ethics Committee recommendations (Decree 86/609/CEE) and were approved by the Animal Experimental Ethical Committee of the University of Antwerp, Antwerp, Belgium (ECD 2016-89). The protocol timeline for the anesthesia and awake scans is presented in Figure 2.

### **Test-Retest Scans**

For the test scans of the anesthesia group ( $n = 8$ , first row of Figure 2), awake mice received an intravenous (iv) injection with 0.2 ml of  $^{18}\text{F}$ -FDG ( $18.5 \pm 0.66\text{ MBq}$ ) in the tail vein. The mice were then placed in their home cages for an awake uptake period of 20 min. Afterwards, the mice were anesthetized and placed on the scanner bed. The acquisition started at 30 min after tracer injection, with a duration of 20 min. Retest scans were performed 7 days after the test scans, following the same scanning protocol

( $^{18}\text{F}$ -FDG,  $19.0 \pm 0.65$ ). The anesthesia scans thus refer to scans performed in a motion-free setup, after the mice had undergone an awake tracer uptake.

Test scans of the awake group ( $n = 8$ , third row of Figure 2) followed the same protocol as the anesthesia group, except for (i) the use of isoflurane anesthesia 20 min prior to tracer injection ( $19.0 \pm 0.44$  MBq) for fixing the point sources (10 min duration) and (ii) no use of anesthesia to perform the PET acquisitions. Retest scans followed the same protocol ( $17.8 \pm 1.08$  MBq) and were performed 7 days after test scans.

### **Memantine Challenge Scans**

Mice from the anesthesia group were scanned 3 days after retest scans (second row of Figure 2). The mice first received an intraperitoneal injection of memantine (30 mg/kg, Sigma Aldrich, UK), after which they were returned to their cages for 30 min. These awake animals then received an iv  $^{18}\text{F}$ -FDG injection ( $18.6 \pm 0.50$  MBq) through the tail vein. The mice were once again returned to their cages for an awake uptake period of 20 min. They were subsequently anesthetized with isoflurane and scanned for a duration of 20 min.

In a similar procedure, the mice in the awake group were scanned 3 days after the retest scans (fourth row of Figure 2) following the same protocol used with the anesthesia group, and with the same exceptions (i and ii) indicated above ( $17.7 \pm 1.99$  MBq).

Two mice from the anesthesia group (retest, memantine scans) and one from the awake group (memantine scan) were not properly injected with tracer or memantine. Additionally, one mouse removed a point source (awake retest scan). These animals were therefore excluded from the analysis.

### **Brain Image Quantification**

All image processing was performed in PMOD 3.6 (PMOD technologies Ltd, Zurich, Switzerland).

First, the brain was cropped from the PET images and rigidly matched to a predefined <sup>18</sup>F-FDG reference template in Waxholm Space (18). The images were then spatially normalized through non-rigid registration. Predefined segmented brain regions in the reference template, delineated from a magnetic resonance image, were used to calculate the mean regional <sup>18</sup>F-FDG uptake (kBq/cc) in the cortex, caudate putamen, thalamus, hippocampus, and cerebellum. Standardized uptake values (SUV) for each brain region were calculated.

In addition, time activity curves (TAC) for each brain region were extracted from the dynamic reconstructions.

### **Statistical Analysis**

The mean SUV and coefficient of variation (COV) for each brain region in the test, retest, and memantine challenge conditions were calculated for the anesthesia and awake groups. Differences between conditions were assessed using two-way ANOVA with Bonferroni correction.

Test-retest variability was calculated by comparing the regional brain uptake in the test and retest scans for each mouse. The intraclass correlation coefficient (ICC) and the Bland-Altman (BA) analysis were calculated for each brain region.

A linear least-squares fit to the regional 20-min TACs (30-50 min <sup>18</sup>F-FDG post injection) was performed. Slopes significantly different from 0 were determined using a *t*-test. Statistical analysis was performed using GraphPad Prism 6.0 (GraphPad Software, California, USA).

### **Motion Analysis**

For awake acquisitions, the average speed of the mouse was calculated based on the point (inside the head circumference) defined by the centroid of the point sources. The distance travelled by the

mouse was calculated for the total duration of the scan. Position histogram heat maps of the animal's locations in the horizontal plane of the scanner FOV were calculated.

## RESULTS

### Brain Image Quantification

Figure 3 shows the regional SUV for all conditions in anesthetized and awake animals. For the anesthetized animals, there is a significant difference ( $p < 0.05$ ) between the memantine and the test and retest conditions in all tested regions, except for the thalamus and cerebellum in the retest condition. For the awake group, there is a highly significant difference ( $p < 0.0001$ ) in all brain regions between the test-retest and the memantine challenge conditions. In the thalamus, the SUV increased by 14.2% ( $p = 0.031$ ) in the anesthesia group, while it increased by 51.5% ( $p < 0.0001$ ) in the awake group. No significant differences were found between test and retest scans. However, there seemed to be a trend towards an increased uptake in the retest scan in the anesthesia group and a less pronounced trend towards a reduced uptake in the retest scan of the awake group (see Supplemental Figures 4 and 5).

Within the anesthesia group, the COV of the cortex are 11.8%, 14.8, and 16.7% in the test, retest, and memantine scans, respectively. For the awake group, the COV of the cortex are 13.8%, 15.3%, and 16% in the test, retest, and memantine scans, respectively. A similar trend can be observed for the other regions. The mean brain regional SUV and COV for all conditions in anesthetized and awake groups are summarized in Table 1.

When comparing anesthetized and awake groups, the mean SUV in test and retest scans tended to be lower for awake animals. No significant differences between the anesthetized and awake mice ( $p > 0.999$  for all brain regions) were found for the memantine challenge. A similar result can be observed in the TAC values for the anesthesia and awake groups, as displayed in Supplemental Figures 1 and 2 for the test and memantine conditions, respectively.

The test-retest variability statistics are presented in Table 2. The ICC in anesthesia scans is in the 0.491-0.629 range for the different brain regions. In the awake scans, the ICC ranges from 0.424-0.555. The bias in the Bland-Altman analysis was largest in the anesthesia group for all brain regions, although the Bland-Altman bias standard deviation is largest in the awake group.

The PET reconstructions after registration to the mouse brain template for a single mouse and the average of all reconstructions in anesthetized and awake mice for the test-retest and memantine challenge conditions are displayed in Figure 4. The spatial resolution of the images of the awake group is lower, as compared to the images of the anesthesia group. On average, the awake images exhibit blurring comparable to anesthesia images filtered with a Gaussian filter with  $\sigma = 0.6$  mm. Both awake and anesthesia scans reveal similar uptake patterns, as well as a memantine-induced change in the uptake pattern. The most striking memantine-induced changes include a reduced uptake in the cerebellum and an increased uptake in the hippocampus, relative to the other parts of the brain.

For the anesthetized animals, TAC slopes decreased ( $p < 0.001$ ) in all regions for all conditions (Fig. 5, Supplemental Figs. 1 and 2). During the 20 min scan, the SUV decreased by an average of 16% and 15% in the anesthesia test and memantine conditions, respectively. For the awake animals, the slopes were not significantly different from zero, except for the caudate putamen, where there was an increase of 7% ( $p = 0.026$ ) in the memantine challenge condition.

### **Motion Analysis of Awake Mice**

Average head speed increased in the memantine challenge condition ( $4.25 \pm 0.67$  cm/s) relative to the test-retest ( $2.09 \pm 0.66$  cm/s) condition. There was a significant ( $p < 0.0001$ ) increase in total distance traveled during the 20-minute scan between the memantine ( $18.2 \pm 5.28$  m) and test-retest ( $6.49 \pm 2.21$  m) conditions. Figure 6 shows horizontal heat maps during the test, retest, and memantine challenge scans for two representative animals. During test and retest scans, mice remained at the same

location for longer periods, changing position sporadically. In contrast, during the memantine challenge scans, mice moved constantly throughout the entire scan, with practically no resting periods. Supplemental Videos 1 and 2 show a mouse during a test scan, and Supplemental Videos 3 and 4 show a mouse in the memantine challenge scan. The entire mouse <sup>18</sup>F-FDG activity projection on the horizontal plane in short time frames (32 ms) is shown in Supplemental Videos 2 and 4.

## DISCUSSION

In this study, the PST method, which was previously developed for awake rat brain PET scanning, was adapted for head motion tracking in awake mice. We adapted the algorithm developed for rat motion tracking to handle the higher moving speed of mice. In previous experiments, rat head moving speed was around 0.5 cm/s (9), while mouse head moving speed was around 2 cm/s in the test-retest experiments and 4 cm/s in the memantine challenge experiments. Another modification compared to rat tracking was the use of a lightweight spacer in order to avoid spillover to the brain.

Similar to awake rat imaging, some loss of spatial resolution can be observed in our awake images. Motion-tracking errors constitute one factor that causes deterioration in the spatial resolution of awake images. For PST, these errors are caused primarily by slipping of the point sources on the skin of the mouse, due to grooming behavior. Grooming might be reduced by familiarizing the mice to the awake scan setup, especially with regard to the markers attached to the fur. A second factor that deteriorates the spatial resolution of awake images is the parallax effect. The position of the brain of an awake mouse is often located in off-center positions, which are closer to the edge of the FOV. In this case, the spatial resolution of the PET camera is lower relative to the centered position of an anesthetized animal.

Despite the loss of spatial resolution in awake images, the regional brain quantification is minimally affected. After filtering the anesthesia images in the three conditions with a Gaussian filter equivalent to the loss of spatial resolution in awake images ( $\sigma = 0.6$  mm), no significant difference was

found in regional brain quantification with respect to the original (unfiltered) image (Supplemental Fig. 3). In addition, the test-retest variability in these awake images was similar to that of scans performed using anesthesia, as quantified with the ICC and the Bland-Altman analysis. In a previous study, Casteels, et al. (19) report on the test-retest variability for <sup>18</sup>F-FDG SUV brain regional quantification in anesthetized mice. The test-retest variability in the current study (e.g., in cortex and following the metric used in (19), variability of 7.64% (anesthesia) and 14.15% (awake)) is lower than that reported in their study (27.74%).

In this study, we considered the irreversible tracer <sup>18</sup>F-FDG, in order to allow comparison between the awake and anesthesia PET acquisitions. Glucose analog <sup>18</sup>F-FDG becomes trapped in the cell upon phosphorylation by hexokinase (20). Given that the anesthesia scans considered a similar awake tracer uptake time as the awake scans, we expected the uptake in the awake and anesthesia scans to be similar. Despite the anticipated similarities, anesthesia continued to have a large effect, as visible in the SUV quantification. First, the uptake in awake mice was lower in test-retest scans, as compared to their anesthetized counterparts. The brief administration of isoflurane 20 minutes prior to <sup>18</sup>F-FDG injection in order to glue the point sources for awake acquisitions might have contributed to this effect (3,4). In future studies, a longer recovery period should be considered after fixing the point sources and prior to tracer injection. In the test-retest scans, the recovery period was only 10 minutes. A longer recovery period is necessary in order to allow brain function to return to its normal state. To this end, we extended the recovery period to 40 min for the memantine challenge study. As a result, only a minimal difference between the awake and anesthetized SUV values (awake <sup>18</sup>F-FDG uptake) was observed at the start of the scan, as could be seen from the regional TACs (Supplemental Fig. 2). If longer recovery periods are required, the user should increase the activity of the point sources to account for the decay time.

In the retest scans compared to the test scans there was a trend towards an increased SUV in the anesthesia group and a decreased SUV in the awake group. If confirmed, these trends might be caused by anesthesia effects and/or differences in stress levels between repeated scanning. Indeed, in rodents it has

been shown that  $^{18}\text{F}$ -FDG uptake quantified by SUV can be altered by repeated measurements (21). While we have allowed a 1-week recovery period between two scans, the repeated scanning might still have contributed to different trends.

We also observed a steady state (slope  $\approx 0$ ) of the TACs during the 20-min scan in awake animals for both the test-retest and memantine conditions. This is similar to results reported by Mizuma, et al. (4) 30 min after tracer injection. In contrast,  $^{18}\text{F}$ -FDG uptake in anesthetized mice decreased during the acquisition (approximately 15% during 20 min) for all conditions. This indicates that, even after an awake uptake period, the changes in  $^{18}\text{F}$ -FDG consumption, induced by isoflurane, exert an effect on the  $^{18}\text{F}$ -FDG signal.

In both the anesthesia and awake groups, we observed an increase of  $^{18}\text{F}$ -FDG regional brain uptake after memantine injection, in comparison to test-retest scans. On average, the difference between the test-retest and memantine challenges was 2.6 time larger for awake scans. This is also reflected in the significance levels, and it can be attributed to the effect of isoflurane. Our results reveal a trend toward increasing  $^{18}\text{F}$ -FDG uptake over time in the awake memantine condition for all regions, with the exception of the cerebellum.

In addition to the imaging, we assessed memantine-induced increased motor activity during PET acquisitions in the awake group. In the memantine challenge, the average mouse speed more than doubled relative to the test-retest condition. Moreover, the total distance travelled was about 3 times longer after memantine injection. The increase in mouse brain glucose uptake (11) has been reported elsewhere, as has the increase in motor activity (12) under memantine challenge. These results demonstrate the tracking algorithm's ability to track the motion of animals in a wide range of speed as well as the ability of the awake imaging to detect memantine induced alterations in  $^{18}\text{F}$ -FDG brain uptake and changes in behavior.

In the present study, we did not measure animal stress. A non-invasive stress quantification method is difficult to implement in freely moving mice and it would most likely affect normal behavior. However, this study involved minimal sources of stress (e.g., awake handling for tracer injections). Although the size of the point sources was small enough to avoid distress in the animals, they seemed to cause mild stress in some mice (as evidenced in constant grooming behavior), while others were apparently unaffected (see e.g. Supplemental Video 1). A training period might further reduce stress in the presence of the point sources.

Although  $^{18}\text{F}$ -FDG was used for validation purposes to compare the resulting images of awake versus anesthetized animals, awake PET scans could be beneficial to other PET tracers. In addition to being a tool for studying the potential effects of anesthesia brain kinetics of PET tracers, PET imaging of freely moving mice is particularly interesting for tracers whose pharmacokinetics might be correlated with animal behavior.

## CONCLUSIONS

In this study, test-retest and memantine-induced brain activation studies were performed in awake, freely moving mice. We generated reliable regional quantification for awake PET acquisitions. This is reflected by slightly lower test-retest reproducibility in awake compared to anesthetized mice, along with very similar coefficients of variation for the two groups. Memantine-induced brain activation shows a clear increase in brain  $^{18}\text{F}$ -FDG uptake relative to unchallenged mice. In addition, the obtained behavioral information during the awake PET acquisitions showed increased motor activity during the memantine challenge. Our proposed PET setup makes it possible to study radiotracer brain uptake in awake animals, thereby ruling out the confounding factor of anesthesia and enabling the simultaneous measurement of animal behavior.

## **DISCLOSURE**

This work was supported by a Research Project (G0A8517N) and Research Grant (1520217N) from the Research Foundation – Flanders (FWO). No potential conflicts of interest relevant to this article exist.

## **ACKNOWLEDGMENTS**

Authors would like to thank Philippe Joye and Caroline Berghmans for the assistance on *in vivo* experiments.

## **REFERENCES**

1. Alstrup AK, Smith DF. Anaesthesia for positron emission tomography scanning of animal brains. *Lab Anim.* 2013;47:12-18.
2. Fueger BJ, Czernin J, Hildebrandt I, et al. Impact of animal handling on the results of 18F-FDG PET studies in mice. *J Nucl Med.* 2006;47:999-1006.
3. Matsumura A, Mizokawa S, Tanaka M, et al. Assessment of microPET performance in analyzing the rat brain under different types of anesthesia: comparison between quantitative data obtained with microPET and ex vivo autoradiography. *Neuroimage.* 2003;20:2040-2050.
4. Mizuma H, Shukuri M, Hayashi T, Watanabe Y, Onoe H. Establishment of in vivo brain imaging method in conscious mice. *J Nucl Med.* 2010;51:1068-1075.
5. Sung KK, Jang DP, Lee S, et al. Neural responses in rat brain during acute immobilization stress: a [F-18]FDG micro PET imaging study. *Neuroimage.* 2009;44:1074-1080.
6. Patel VD, Lee DE, Alexoff DL, Dewey SL, Schiffer WK. Imaging dopamine release with Positron Emission Tomography (PET) and (11)C-raclopride in freely moving animals. *Neuroimage.* 2008;41:1051-1066.

- 7.** Schulz D, Soutekal S, Junnarkar SS, et al. Simultaneous assessment of rodent behavior and neurochemistry using a miniature positron emission tomograph. *Nat Methods*. 2011;8:347-352.
- 8.** Kyme AZ, Zhou VW, Meikle SR, Baldock C, Fulton RR. Optimised motion tracking for positron emission tomography studies of brain function in awake rats. *PLoS One*. 2011;6:e21727.
- 9.** Miranda A, Staelens S, Stroobants S, Verhaeghe J. Fast and accurate rat head motion tracking with point sources for awake brain PET. *IEEE Trans Med Imaging*. 2017;36:1573-1582.
- 10.** Homberg JR, Wohr M, Alenina N. Comeback of the rat in biomedical research. *ACS Chem Neurosci*. 2017;8:900-903.
- 11.** Dedeurwaerdere S, Wintmolders C, Straetemans R, Pemberton D, Langlois X. Memantine-induced brain activation as a model for the rapid screening of potential novel antipsychotic compounds: exemplified by activity of an mGlu2/3 receptor agonist. *Psychopharmacology (Berl)*. 2011;214:505-514.
- 12.** Fredriksson A, Danysz W, Quack G, Archer T. Co-administration of memantine and amantadine with sub/suprathreshold doses of L-Dopa restores motor behaviour of MPTP-treated mice. *J Neural Transm (Vienna)*. 2001;108:167-187.
- 13.** Bao Q, Newport D, Chen M, Stout DB, Chatzioannou AF. Performance evaluation of the inveon dedicated PET preclinical tomograph based on the NEMA NU-4 standards. *J Nucl Med*. 2009;50:401-408.

- 14.** Rahmim A, Lenox M, Reader AJ, et al. Statistical list-mode image reconstruction for the high resolution research tomograph. *Phys Med Biol*. 2004;49:4239-4258.
- 15.** Reader AJ, Julyan PJ, Williams H, Hastings DL, Zweit J. EM algorithm system modeling by image-space techniques for PET reconstruction. *IEEE Trans Nucl Sci*. 2003;50:1392-1397.
- 16.** Rahmim A, Dinelle K, Cheng JC, et al. Accurate event-driven motion compensation in high-resolution PET incorporating scattered and random events. *IEEE Trans Med Imaging*. 2008;27:1018-1033.
- 17.** Angelis G, Bickell M, Kyme A, et al. Calculated attenuation correction for awake small animal brain PET studies. *IEEE Nucl Sci Symp Conf Rec*. 2013.
- 18.** Johnson GA, Badea A, Brandenburg J, et al. Waxholm space: an image-based reference for coordinating mouse brain research. *Neuroimage*. 2010;53:365-372.
- 19.** Casteels C, Vunckx K, Aelvoet SA, et al. Construction and evaluation of quantitative small-animal PET probabilistic atlases for [(1)(8)F]FDG and [(1)(8)F]FECT functional mapping of the mouse brain. *PLoS One*. 2013;8:e65286.
- 20.** Reivich M, Kuhl D, Wolf A, et al. The [18F]fluorodeoxyglucose method for the measurement of local cerebral glucose utilization in man. *Circ Res*. 1979;44:127-137.

**21.** Deleye S, Verhaeghe J, Wyffels L, et al. Towards a reproducible protocol for repetitive and semi-quantitative rat brain imaging with (18) F-FDG: exemplified in a memantine pharmacological challenge. *Neuroimage*. 2014;96:276-287.

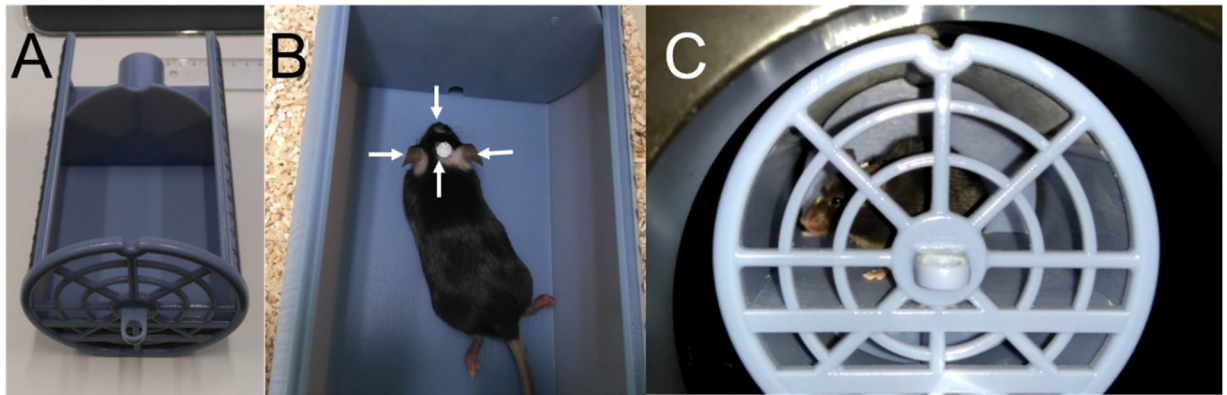


FIGURE 1. (A) Holder (top cover removed) in which the mouse was placed during acquisitions. (B) Mouse with fixed point sources, indicated by the white arrows. (C) Mouse inside the holder during the PET acquisition.

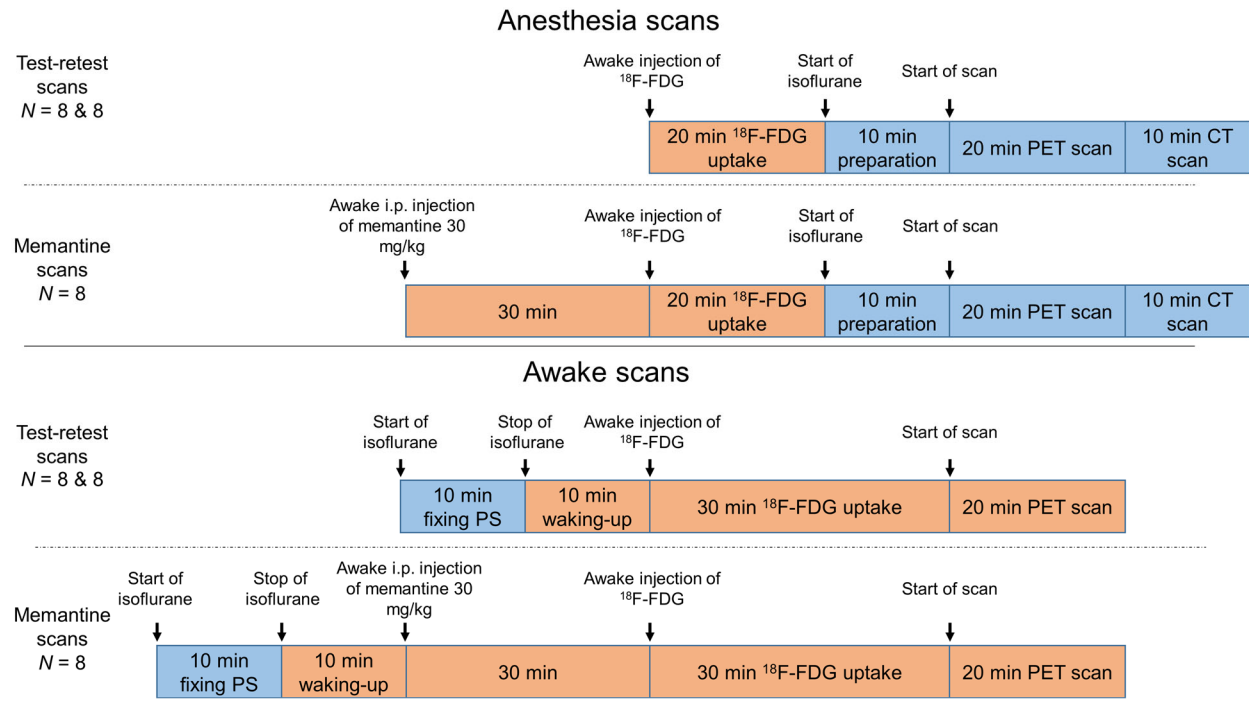


FIGURE 2. Scanning protocol for anesthetized and awake animals for test, retest, and memantine challenge conditions. PS = point sources, blue = anesthesia, orange = no anesthesia.

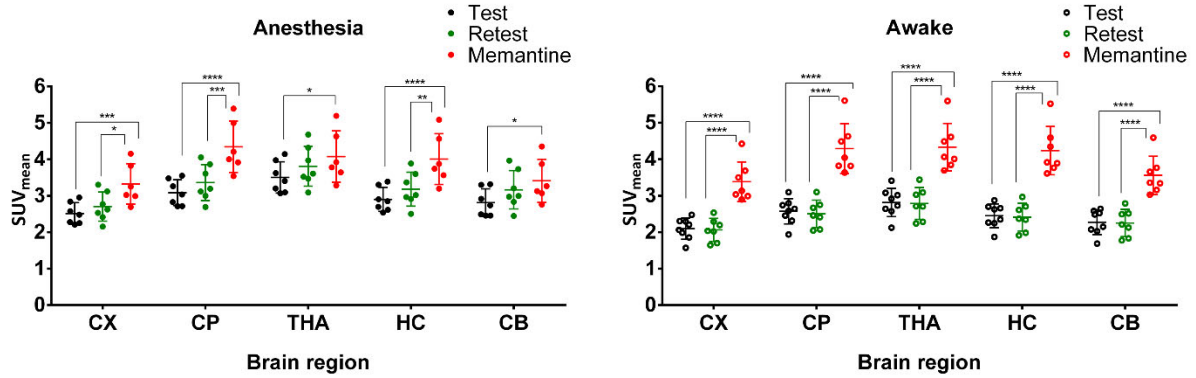


FIGURE 3. Scatter plot of SUV for different brain regions in test, retest, and memantine challenge conditions for both the anesthesia and awake groups. Significance level  $p^* < 0.05$ ,  $p^{**} < 0.01$ ,  $p^{***} < 0.001$ ,  $p^{****} < 0.0001$ . CX: cortex, CP: caudate putamen, TH: thalamus, HC: hippocampus, CB: cerebellum.

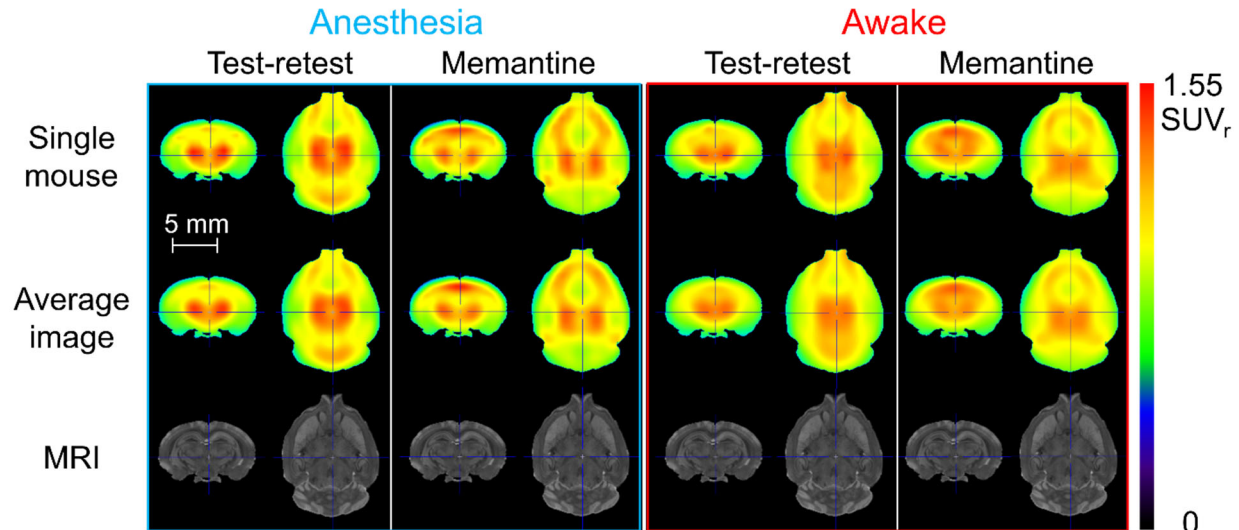


FIGURE 4. Anesthesia and awake images for a single mouse and averaged over all mice from each group. MRI template images are included as an anatomical reference. The test-retest and memantine challenge conditions are displayed for each group. Image values are normalized to whole brain uptake for visualization purposes (SUV ratio, SUV<sub>r</sub>).

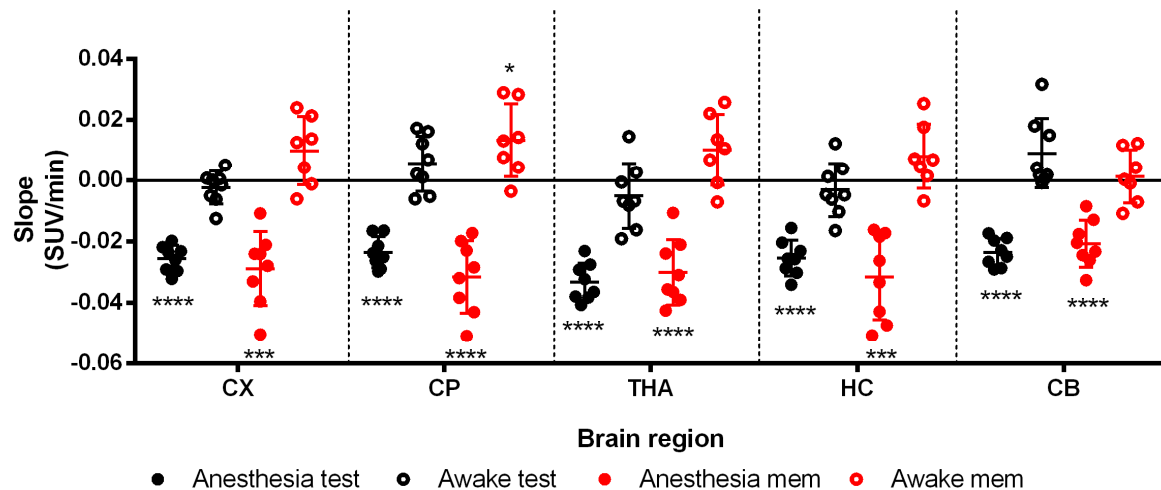


FIGURE 5. Slopes of the linear least squares fit to the TACs for the anesthetized and awake groups in the test and memantine challenge conditions. Significance level  $p^* < 0.05$ ,  $p^{***} < 0.001$ ,  $p^{****} < 0.0001$ .

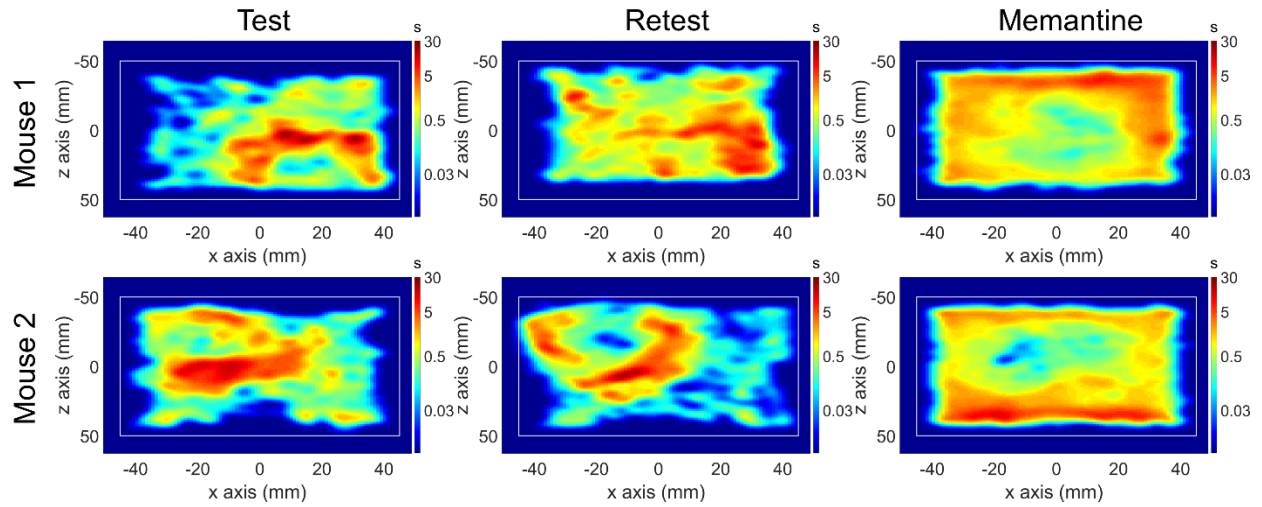


FIGURE 6. Position histogram (heatmap) on the horizontal plane for 2 mice during the test, retest, and memantine challenge acquisitions. Logarithmic time color scale in seconds. Platform limits are represented as a white rectangle.

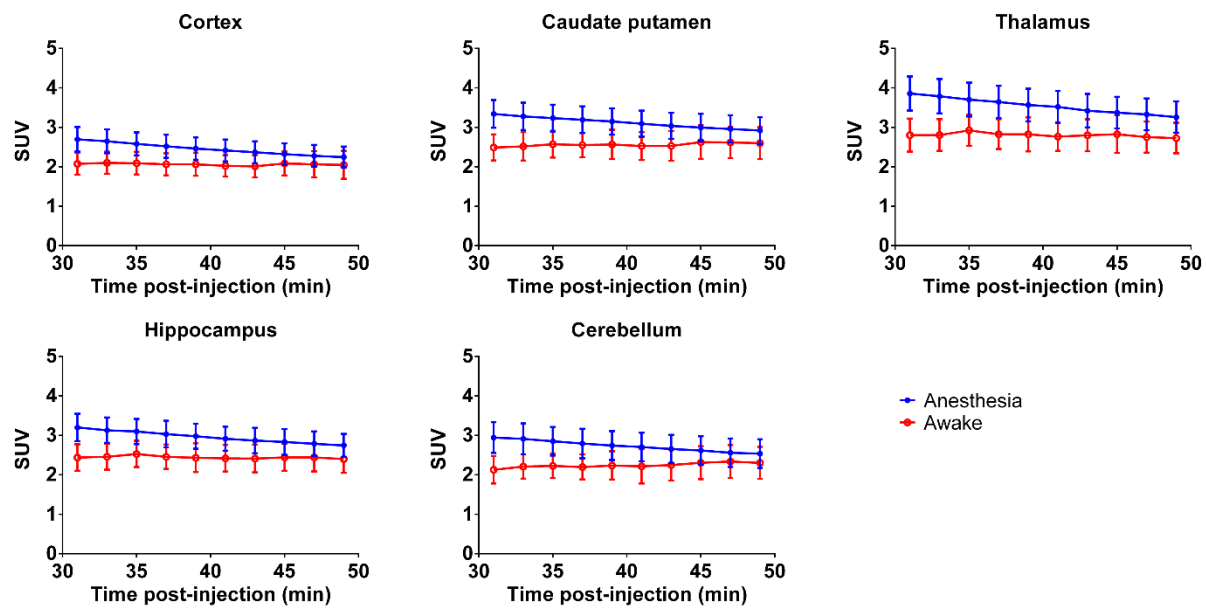
TABLE 1. Mean regional SUV and COV for the different conditions in anesthetized and awake animals.

	Brain region	Mean (SUV)			COV (%)		
		T	RT	MEM	T	RT	MEM
Anesthesia	CX	2.51	2.70	3.32	11.8	14.8	16.7
	CP	3.08	3.36	4.34	11.4	14.7	16.2
	TH	3.50	3.81	4.08	12.2	14.4	17.3
	HC	2.90	3.18	4.01	11.4	14.7	17.4
	CB	2.81	3.16	3.41	13.5	16.6	17.3
Awake	CX	2.10	2.06	3.38	13.8	15.3	16.0
	CP	2.57	2.50	4.29	13.5	15.0	16.0
	TH	2.81	2.79	4.33	13.8	15.6	15.0
	HC	2.45	2.41	4.24	13.3	15.8	15.6
	CB	2.27	2.25	3.56	14.9	16.6	14.8

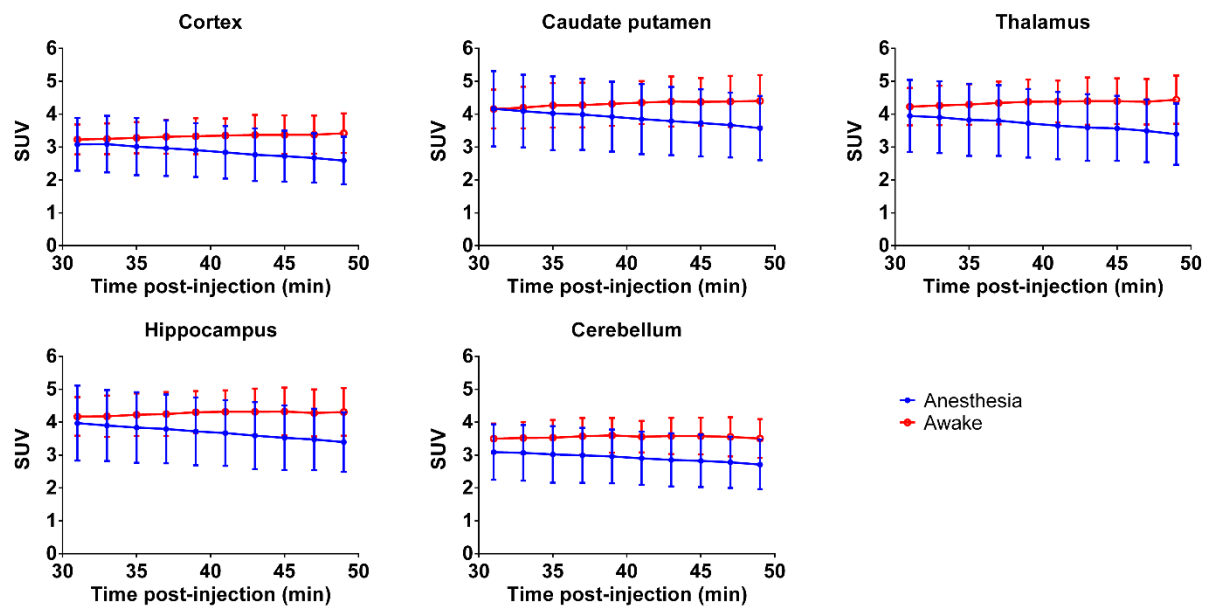
CX: cortex, CP: caudate putamen, TH: thalamus, HC: hippocampus, CB: cerebellum. T: test, RT: retest, MEM: memantine.

TABLE 2. ICC and Bland-Altman bias (bias) and bias standard deviation (bias SD) for the test-retest comparison of regional brain SUV in anesthetized and awake groups.

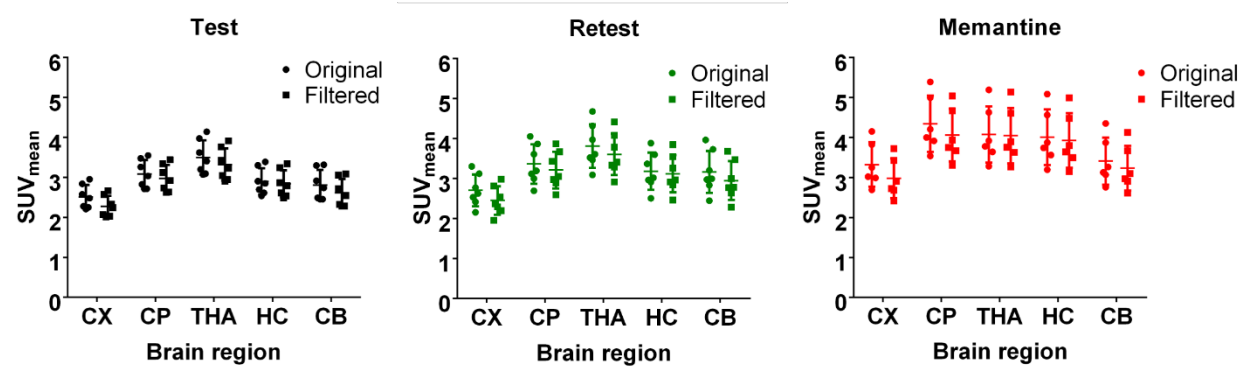
	Brain region	ICC	bias (%)	bias SD
Anesthesia	CX	0.629	-6.94	5.90
	CP	0.553	-8.25	5.94
	TH	0.580	-8.15	5.35
	HC	0.505	-8.81	7.39
	CB	0.491	-11.4	6.48
Awake	CX	0.488	0.90	20.0
	CP	0.481	2.34	18.6
	TH	0.424	-0.04	19.2
	HC	0.555	0.43	19.4
	CB	0.444	-0.53	21.4



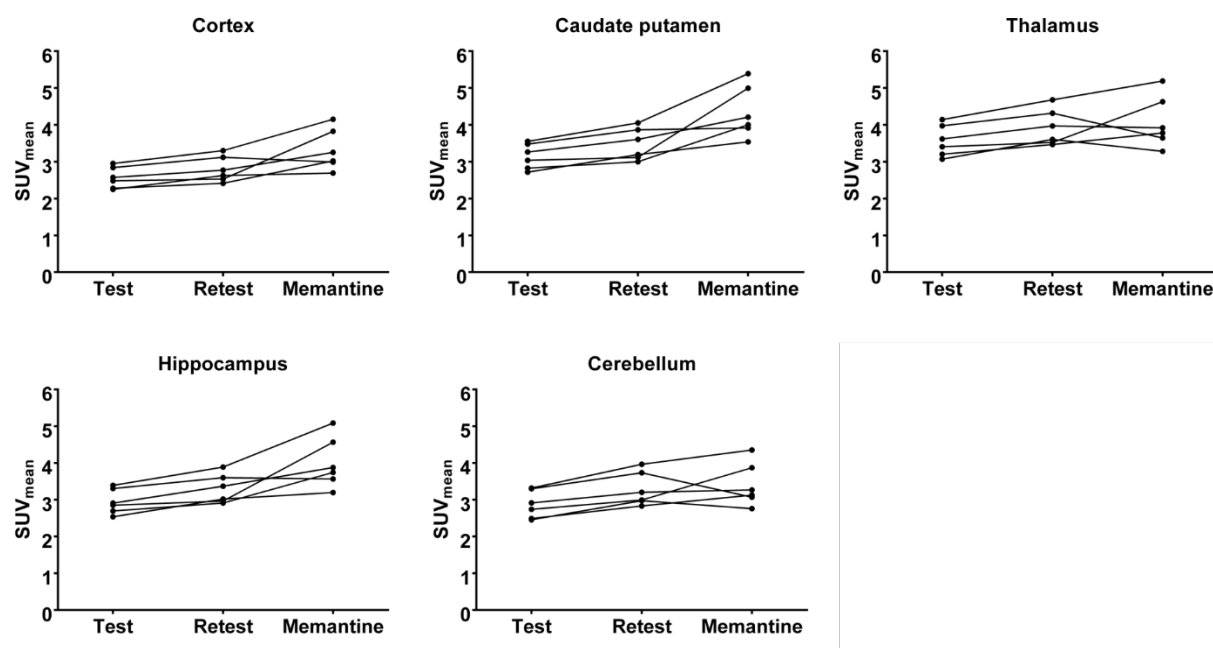
Supplemental Figure 1. Mean  $\pm$  standard deviation time activity curves during the test scans for the different brain regions in the anesthesia (blue) and awake (red) group mice. Frame duration is 2 minutes.



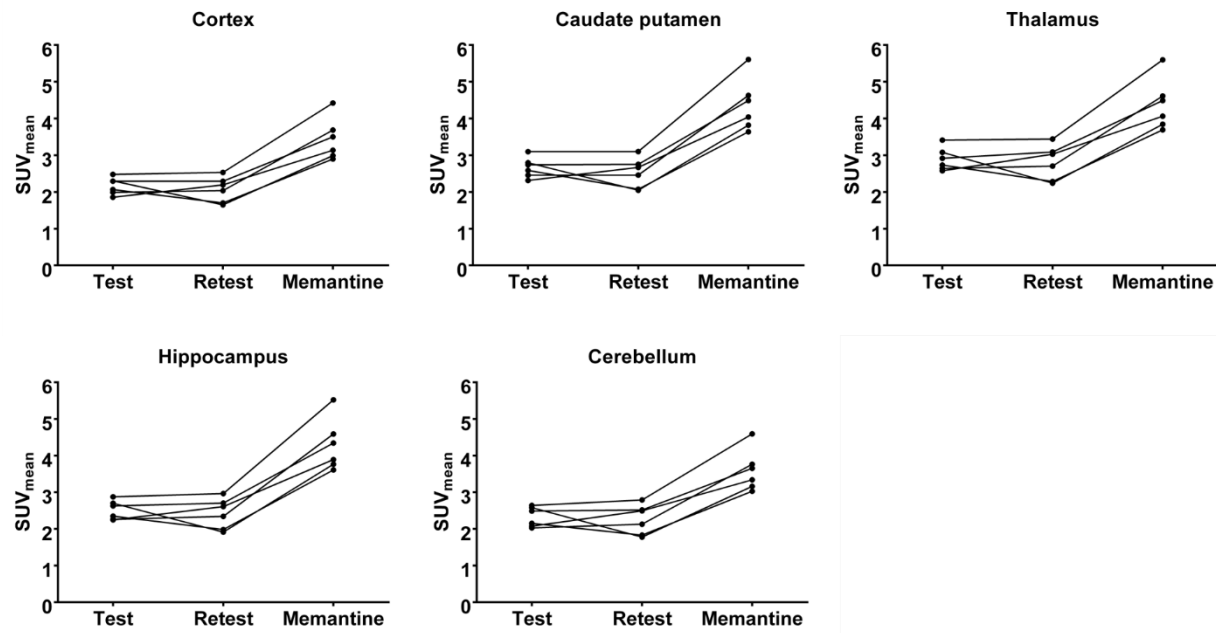
Supplemental Figure 2. Mean  $\pm$  standard deviation time activity curves during the mémantine challenge scans for the different brain regions in the anesthesia (blue) and awake (red) group mice. Frame duration is 2 minutes.



Supplemental Figure 3. Scatter plot of SUV for different brain regions for the test, retest and memantine condition for the anesthesia group original images (Original) and when smoothed with a Gaussian filter with  $\sigma = 0.6$  mm (Filtered). No significant difference was found between regional brain quantification in original and filtered images in any case. CX: cortex, CP: caudate putamen, TH: thalamus, HC: hippocampus, CB: cerebellum.



Supplemental Figure 4. Spaghetti plots of the SUV for different brain regions in the anesthesia group for the test, retest and memantine condition.



Supplemental Figure 5. Spaghetti plots of the SUV for different brain regions in the awake group for the test, retest and memantine condition.